Open Plasma Science

Vol. ICPIG 2025, No. 2 (2026)

SPECIAL ISSUE

History
Received August 25, 2025
Revised October 23, 2025
Accepted October 31, 2025
Published February 11, 2026

Identifiers
DOI 10.46298/ops.16405
HAL -
ArXiv -
Zenodo 17423193

Supplementary Material
-



# Modeling of evaporation of macroparticles of vacuum arcs by an electron beam

Iryna Litovko[1,2], Martin Rudolph[1], Andre Anders[1,3], and Alexey Goncharov[4]

[1]Leibniz Institute of Surface Engineering (IOM), Leipzig, Germany
[2]Institute for Nuclear Research NAS of Ukraine, Kyiv, Ukraine
[3]Felix Bloch Institute of Solid State Physics, Leipzig University, Leipzig, Germany
[4]Institute of Physics, NAS of Ukraine, Kyiv, Ukraine

## Abstract

The evaporation of droplets in an arc plasma flow under the action of an electron beam self-consistently formed in a plasma-optical filter is considered under the conditions of direct heating of microdroplets by beam electrons. Analytical modeling shows that droplets $\leq 1$ $\mu$m in size can be completely evaporated over time scales typical for cathodic arc deposition systems. It is shown that small microdroplets evaporate more intensively. The lower limit working points in terms of plasma electron density, and the electron energy and density of the injected energetic electrons required for droplet evaporation are found.

**Keywords**— plasma optics, vacuum-arc discharge, droplets, fast electrons, film deposition, droplet evaporation

* Corresponding author: iryna.litovko@kinr.kyiv.ua

Cite as: Litovko *et al.*, Modeling of evaporation of macroparticles of vacuum arcs by an electron beam, *Open Plasma Science* ICPIG 2025, 2 (2026), doi: 10.46298/ops.16405

# Contents



## 1 Introduction

Modern industrial technological processes, such as the production of integrated circuits, devices on a chip, modification of the surface layer for various purposes, require efficient and reliable nano production means. The quality and precision of manufacturing such products must be complemented by maximum productivity. Ion-plasma sources of the Metal Vapor Vacuum Arc (MEVVA)-type, using a vacuum-arc discharge [I.G94], are widely and effectively used in the application of protective and functional coatings and modification of surface properties. However, the generation of metal plasma in a vacuum arc discharge as a result of cathode erosion is always accompanied by the formation of microdroplets of the cathode material, which is a significant limitation that prevents the creation of high-quality coatings that are uniform on the nanometer scale. In areas such as optics and microelectronics, the presence of macroparticles (droplets) is a significant obstacle to the production of high-quality films, since the thickness of the deposited films is 0.01 $\mu$m to 1 $\mu$m, which is on the order of the size of the droplets.

The problem of removing droplets using filtration of plasma flow is widely covered in scientific and technical literature [Zim05, And00, AAS07]. Modern filters and methods for removing these droplets are based on various forms of selection primarily mechanical and electrophysical filters [Zim05, And00]. These filters effectively remove droplets larger than 1 $\mu$m without significant loss of ion-vapor flow particles. However, the use of these filters to remove droplets with smaller sizes leads to a significant (several times) decrease in the flux of the metal plasma onto the processed products. This reduces the effects from energetic deposition that is usually wanted from such an erosive deposition source. Another way to remove droplets from a vacuum-arc plasma stream is the use of magnetic filters of various configurations, using a significant difference in the masses of plasma particles (ions, electrons) and microdroplets [AAS07]. A higher droplet removal rate requires a more complex design, though, increasing the cost of the process. At the same time, neutral metal atoms are lost in such a filter in addition, which results in a loss of deposition rate, with negative impact on productivity. Thus, a characteristic feature of modern macroparticles filters is a significant loss (often more than 75%) of material in the plasma flow. That is, modern filtration methods compromise the typically high deposition rate of ion-vapor flow generation inherent in erosive plasma sources. This motivates the quest for alternative methods for droplet removal that do not lead to losses in the productivity of the ion-plasma coating deposition process.

A possible way to achieve this is not to remove the droplets from the plasma flow, but to evaporate them in the plasma flow. Anders [And97, And99] discussed and analyzed this idea using balance equations. He

concluded that the evaporation of droplets in an arc plasma flow without an additional energy source would not be possible. Such an additional source of energy can be pumping energy into the arc plasma flow with a high-energy electron beam, ensuring evaporation and destruction of the droplet. The Institute of Physics of the National Academy of Sciences of Ukraine (IP NASU) proposed to build a filtration system that does not involve removing the droplet phase from the plasma flow, but, on the contrary, uses the droplet phase as an additional source to the plasma flow and thereby increases the productivity of the coating system and adding an electron beam to the plasma system ensures the evaporation and destruction of the droplet [FMG14, Gon16]. To remove droplets from the flow of dense metal plasma, a new approach using plasmadynamic systems, such as electrostatic plasma lenses (PL) and hollow cathode (HC) discharge systems, was proposed and studied [AVA+19]. These systems generate an energetic electron beam that can effectively vaporize and remove droplets.

However, for the most effective application of the proposed systems, it is necessary to understand the fundamental physical mechanisms affecting microparticles in dense dusty plasma during their passage through plasma-dynamic systems with fast electrons. For the calculation, we are using copper as an exemplary material due to the availability of material properties. It also has a moderate melting point which makes an ideal test candidate for this type of study. Moreover, copper is an important material in particular in microelectronics (for example see [SS00]).

## 2 Plasma-optical filter

Let us consider a plasma-optical filter [AVA+19], in which additional energy for the evaporation of droplets is pumped by an electron beam, that created self consistently. The schematic picture is shown in figure 1. The arc plasma flow with the droplet fraction is formed by a vacuum arc source with cathode C and anode A. The plasma flow expands from the cathode C and passes through the diaphragm D. After the diaphragm, the flow enters the plasma-optical filter. The plasma-optical filter is a hollow cylinder $C_1$, length L ($\sim$17$\div$20 cm) and radii R ($\sim$3.5 cm), to which a negative voltage is applied. In the vicinity of this cylinder, this leads to the formation of a layer of thickness $\Delta << \rho_e = eE_r/m_e{\omega_{He}}^2$ and a large radial electric field $E_r$, near the electrode. It should be noted that the system is placed in a magnetic field (of 0.02-0.04 T) of short coil or system of permanent magnets where the inequalities $\rho_{He} << 2R << \rho_{Hi}$ shall be met. Here, $\rho_{He}$ and $\rho_{Hi}$ are the Larmor radii of electrons and ions. In this system, the electrons are magnetized while the ions are not magnetized. The electron beam (labelled "e-beam" in figure 1) is formed as a result of secondary ion-electron emission when the inner surface of the central cylindrical electrode ($C_1$), to which voltage (from -1 keV to -3.5 keV) is applied, is bombarded by peripheral ions of the plasma flow (shown by arrows in figure 1), that accelerate in the layer $\Delta$ in the direction of the central electrode $C_1$.

This electron beam has velocity $V_b = (2eU/m_e)^{1/2}$ and current density $j_b = \gamma j_i$, where $\gamma \sim 0.1$ is the coefficient of secondary ion-electron emission. This high energy electron beam is accelerated by an applied potential difference approximately radially in the direction of the system axis. Thus, the electron beam formed on the inner surface of the central cylindrical electrode of the plasma-optical filter adds to the propagating plasma flux a significant portion of the energy that exceeds all energy accumulated in the plasma ions and electrons. Note also, that in the depth of the plasma flow, in its main volume, due to the polarization of the plasma flow during its interaction with the magnetic field, a significantly smaller radial electric field is formed, which controls the properties of the plasma flow and limits the expansion of the flow along the radius.

For the effective use of the proposed filter, it is necessary to understand the physical mechanisms of heating droplets in a dense dusty plasma with a high-energy electron population, which would allow finding the optimal operating parameters of the plasma filter. Here, we are interested in the conditions necessary to evaporate macroparticles. We therefore neglect the loss of copper ions from the cathodic arc process due to the acceleration toward the secondary cathode. In the following, we assume ions to be at least doubly charged,

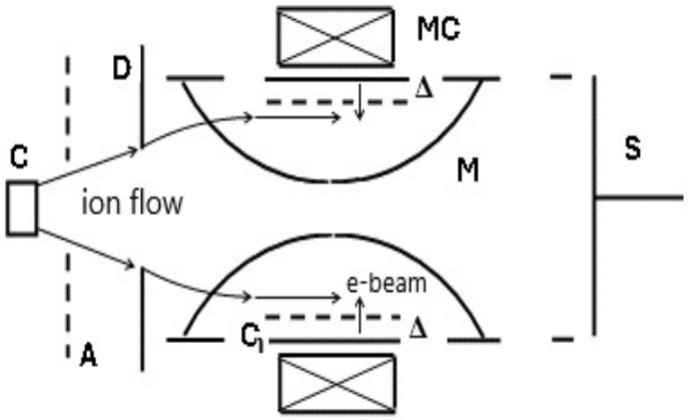


**Figure 1:** Schematic of the plasma-optical filter: C - cathode, A - anode, D - diaphragm, MC - magnetic coil, M - magnetic field lines, S - substrate, $C_1$ - cylindrical electrode that forms an electron beam under the action of secondary ion electron emission.

because in a cathodic arc process most ions are usually multiply charged. The plasma conditions used below are typical for those of a cathodic arc plasma. According to the estimates, for typical parameters of a plasma flux formed by a vacuum-arc source, the ion energy in the flux is $\varepsilon_i = 20 - 60$ eV and ion temperature is 1 eV, the electron plasma temperature $T_e$ and their density $n_0$ are $T_e = 2 - 4$ eV, $n_0 = 10^{10}$ to $10^{12}$ $cm^{-3}$, respectively. We thus assume that the dense plasma of the cathode spot has already considerably expanded which is accompanied by a cooling of the electron population.

The density of macroparticles can be found by comparing the masses of the ionic component and the droplet component, since it is known that the mass of macroparticles is comparable to the mass of ions, and sometimes even exceeds it. From the condition of equality of masses, we obtain an estimate of the particle density of $n_{dr} \sim 3 \cdot 10^3$ cm$^{-3}$. Assuming a droplets velocity of 100 m/s, we calculate the residence time of the macroparticle in the filter to be 2 ms. This is the time during which a particle needs to be completely evaporated in order to not be immersed into the growing thin film onto the substrate.

## 3 Description of the mathematical model of droplet evaporation

The rate of evaporation of a droplet is determined by its temperature, therefore, to determine how quickly the evaporation process will occur, it is necessary to know the temperature of the droplet, which changes during its stay in the discharge. On the other hand, the temperature of the droplet is determined from the balance of energy absorbed and lost by the droplet, but this is also accompanied by a change in the charge of the droplet. The charge that the particle acquires in the plasma medium, is a fundamental characteristic of a droplet, that depends on the plasma parameters. It is the charge that determines the movement of the droplet in the plasma and the possibility of its destruction and disappearance from the plasma flow.

In the absence of an electron beam, only a current of plasma electrons ($I_e$) and ions ($I_i$) come to the macroparticles, which affects the heating and charge of the droplet. Secondary emission of electrons from the surface of the droplet can be neglected in comparison to the plasma electron and ion currents arriving at the droplet. However, the equilibrium droplet temperature in this case is not high enough for intense droplet evaporation. One example is that by Boxman and Goldsmith [BG92], who found that copper droplets lose 30% of their initial mass as the result of ion bombardment. This example illustrates that it is difficult or impossible

to quickly evaporate macroparticles without an additional energy source.

The presence of an electron beam in the plasma flow introduces significant changes both to the thermal balance equation of the droplet and to the process of its charging. Beam electrons not only bring additional energy and charge to the droplet but also induce processes that remove energy and charges from the droplet such as secondary electron emission as well as thermal and/or field emission. A high-energy electron beam is also capable of charging a droplet to a critical charge at which Rayleigh decay occurs, which can take on a cascade character and gives us another opportunity to remove droplets from the flow. In addition, indirect heating of droplets is possible when electron beams heat plasma electrons, which in turn transfer energy to the droplet. However, here we limited ourselves to direct heating of the droplet by an electron beam, since this is justified by looking at the expressions for collisions between beam electrons and plasma electrons: $\nu_{b\_e} \approx 6.5 \cdot 10^{-6}\ \varepsilon_b^{-3/2} n_e \Lambda_{ee}$ [SJ06], where $\varepsilon_b$ is electron beam energy, $n_e$ is the plasma electron density, $\Lambda_{ee}$ is the Coulomb logarithm. The frequency of electron beam absorption by a droplet can be expressed as: $\nu_{b\_dr} = \pi r_{dr}^2 n_{dr} (2\varepsilon_b/m_e)^{1/2}$, where $r_{dr}$ is the droplet radius, $n_{dr}$ is the droplets density, and $m_e$ is the electron mass. For the initial considerations we use the values $\varepsilon_b = 3,000$ eV, $n_e = 10^{12}$ cm$^{-3}$, $n_{dr} = 10^3$ cm$^{-3}$, $V_{dr} \sim 100$ m/s, $\Lambda_{ee} = 10$. We obtain $\nu_{b\_e} = 0.4 \cdot 10^3$ s$^{-1}$ and $\nu_{b\_dr} = 10^5$ s$^{-1}$, thus $\nu_{b\_dr} >> \nu_{b\_e}$, and we conclude that the energy contribution of direct heating of droplets by an electron beam significantly exceeds the contribution from indirect heating. Thus, we see that in this case it is necessary to consider a system of three interrelated differential equations: the energy balance equation, the current balance equation, and the evaporation rate equation.

The energy balance equation can be written as:

$$M_{dr} c \frac{dT_{dr}}{dt} = \sum Q_{in} - \sum Q_{out} \quad , \tag{1}$$

where c is the specific heat capacity of the drop material, $M_{dr}$ and $T_{dr}$ are the mass and temperature of the droplet, and $Q_{in}$ and $Q_{out}$ are the energy fluxes to and from the drop, respectively.

The current balance equation has the form:

$$4\pi\varepsilon_0 r_{dr} \frac{d\varphi_{dr}}{dt} = \sum I_{in} - \sum I_{out} \quad , \tag{2}$$

where $r_{dr}$ and $\varphi_{dr}$ are the radius and potential of the droplet, and $I_{in}$ and $I_{out}$ are the currents to and from the drop, respectively.

To describe the rate of the evaporation process, we can use the Hertz-Knudsen relation in the second term of the right-hand side:

$$\frac{dM_{dr}}{dt} = \frac{I_i}{e} m_i - 4\pi r_{dr}^2 \cdot \gamma_a m_a \quad , \tag{3}$$

Where $I_i$ - ion current to drop, $m_i$ and $m_a$ - mass of ion and atom, $\gamma_a$ - the evaporation rate, which determines the number of atoms evaporated from a unit of surface during a unit of time, that has next form [MGM77]:

$$\gamma_\alpha = \frac{\alpha_k p(T_{dr})}{\sqrt{2\pi m_a k T_{dr}}} \tag{4}$$

$\alpha_k$ is the accomodation coefficient equal to the probability that when a vapor molecule hits the surface of the drop, it will not be reflected, $p(T_{dr})$ is the equilibrium saturated vapor pressure of the evaporating droplet material, which depends on the temperature $T_{dr}$ on the surface of the droplet.

For the vapor pressure $p(T)$, included in $Q_{vap}$, we use the following equation [Arb15]:

$$\ln p(T) = A + \frac{B}{T} + C \ln(T) + DT + ET^2 \tag{5}$$

where A, B, C, D, E are material-dependent coefficients. The pressure of saturated vapors depends not only on the temperature but also on the radius of curvature of the surface over which they are formed. For a spherical drop surface, we can use for vapor pressure the Ostwald–Freundlich equation:

$$p_{vap.sph} = p(T) \exp\left(\frac{2\sigma V_m}{r_{dr} RT}\right) \tag{6}$$

where $V_m$ is the molar volume, and R is the universal gaz constant, $p(T)$ - pressure for a flat surface (equation 5).

To calculate the currents, we used the Orbital-motion-limited theory (OML) [MSL26]. The condition for applying the OML theory for describing the charging of a droplet contained in a plasma with a magnetic field has the following form: $r_{dr} << \lambda_D << \rho_{He}$, where $\lambda_D$ - Debye length. This condition is fulfilled for a magnetic field with a strength of less than 0.03 T and a plasma with a density of $n_0 = 10^{10}$ cm$^{-3}$ to $10^{12}$ cm$^{-3}$ and electron temperature $T_e = 3 - 10$ eV. According to OML theory, the currents $I_{in}$ from equation 2 corresponding to the currents arriving at the droplet are described as follows. From plasma electrons to droplet:

$$I_e(r_{dr}) = \pi r_{dr}^2 e n_e V_{Te} \exp\left(-\frac{e\varphi_{dr}}{kT_e}\right), \tag{7}$$

from ions is

$$I_i(r_{dr}) = \pi r_{dr}^2 e n_i V_{ib} \left(1 - \frac{e\varphi_{dr}}{\varepsilon_{ib}}\right), \tag{8}$$

and the current of energetic beam electrons is:

$$I_{eb}(r_{dr}) = \pi r_{dr}^2 e n_b V_{eb} \left(1 - \frac{e\varphi_{dr}}{\varepsilon_{eb}}\right). \tag{9}$$

Here $V_{Te}$, $V_{ib}$ and $V_{eb}$ are the velocities of plasma electrons, ions and beam electrons, respectively. $I_{out}$ include emission currents - the secondary electron emission current is equal to [Ste57, BF69]:

$$\begin{gathered} I_{see}(r_{dr}) = \delta_{see} I_b(r_{dr}), \\ \delta_{see} = 7.4\delta_m \frac{\varepsilon_{eb}}{\varepsilon_{max}} \exp\left(-2\sqrt{\frac{\varepsilon_{eb}}{\varepsilon_{max}}}\right). \end{gathered} \tag{10}$$

For the thermo-field emission in the region of dominating thermionic emission current, we use the Murphy-Good equation, which is suitable without limitation on the values of electric field strength and temperature Hantzsche [Han82, MG56]:

$$\begin{gathered} I_{e,th} = 4\pi r_{dr}^2 T_{dr}^2 \frac{e m_e}{2\pi^2 \hbar^3} \frac{\pi h_0}{\sin(\pi h_0)} \exp\left(-\frac{e\left(\Phi - \sqrt{\frac{eE}{4\pi\varepsilon_0}}\right)}{k_B T_{dr}}\right) \\ h_0 = \left(\frac{E\hbar^4}{m_e^2 e^5}\right)^{1/4} \frac{e\sqrt{\frac{eE}{4\pi\varepsilon_0}}}{\pi k_B T_{dr}}. \end{gathered} \tag{11}$$

Here E-electric field on the surface of the droplet. For E we take the approximation $E = \varphi_{dr}/r_{dr}$. In our case, we have $\lambda_D >> r_{dr}$ that justifies using this approximation.

The energy flux $Q_{in}$ in equation 1 included fluxes from primary electrons, ions and beam electrons $Q_e$, $Q_i$ and $Q_{eb}$ respectively, which heat the droplet are equal to:

$$\begin{gathered} Q_e = I_e(2k_BT_e + \Phi_{Cu})/e, \\ Q_i = I_i(2k_BT_i + (\varepsilon_{vap} + \varepsilon_{ex} + \varepsilon_i) + e\varphi_{dr} - \Phi_{Cu})/e, \\ Q_{eb} = I_{eb}(\varepsilon_b + \Phi_{Cu})/e. \end{gathered} \tag{12}$$

The energy flux $Q_{out}$ included fluxes $Q_{rad}$, $Q_{ee}$, $Q_{e,th}$, $Q_{vap}$ and $Q_{hex}$ in equation 1, corresponding to radiation, secondary electron emission, thermal (field-)electron emission, evaporation and heat exchange, cool the droplet. They are equal to :

$$\begin{gathered} Q_{rad} = 4\pi r_{dr}^2 \alpha \sigma_{SB} T_{dr}^4, \\ Q_{ee} = I_{ee}(k_BT_e - \Phi_{Cu})/e, \\ Q_{e,th} = I_{e,th}(2k_BT_{dr} - \Phi_{Cu})/e, \\ Q_{vap} = 4\pi r_{dr}^2 \gamma_a (\varepsilon_{vap} + 2k_BT_{dr})/e, \\ Q_{hex} = 4\pi r_{dr}^2 k n_g v_{T,a}(T_{dr} - T_g). \end{gathered} \tag{13}$$

$\Phi_{Cu}$ in equations 12 and 13 is the work function of material in eV (4.5 eV for copper), $\varepsilon_{vap}$ is the energy of vaporization of one atom, $\varepsilon_{ex}$ is the energy of excitation bound electrons, $\varepsilon_i$ is the ionization energy, $\alpha$ is the emissivity of the droplet material and $\sigma_{SB}$ is the Stefan-Boltzmann constant. $n_g$, $T_g$ are surrouding gas density and temperature respectively.

It should also be noted that the distinctive feature of the system of equations 1-3, is its stiffness. Therefore, for the numerical solution of this system, an algorithm with a variable step and a variable order was chosen, based on the inverse differentiation formulas of the first to fifth order. The Jacobian matrix, necessary for the operation of the algorithm, was calculated by the method of numerical differentiation. As studies show [SR97, BD83], this algorithm effectively finds solutions for this type of system with good accuracy.

The initial temperature of the macroparticles is taken to be the melting temperature of the bulk material (for copper it equals 1357 K), and the initial potential is taken to be the negative potential equal in absolute value to the temperature of the plasma electrons ($T_e = 3$ eV), and we assume that the ion density is approximately equal to the electron density $n_i \approx n_e = n_0$ (quasi-neutrality condition). Typical parameters of the plasma flow formed by the vacuum arc source, given above, are also used as parameters for solving the equations.

## 4 Results

There are two main mechanisms that can affect the destruction of a droplet under the action of an electron beam - these are Rayleigh decay and evaporation. Evaporation occurs at any temperature, but at a higher temperature it occurs faster. It is important that it exceeds the temperature at which $Q_{vap}$ becomes greater than $Q_{rad}$ (for copper this is about 1800 K). Rayleigh decay - when the droplet receives a charge exceeding the Rayleigh limit ($q_R = 8\pi\sqrt{\varepsilon_0 \sigma r_{dr}}$) [HS63]. It is important to understand which mechanism and under what conditions will play a decisive role. Therefore, one of the main questions is to what temperature the electron beam can heat the droplet and what charge the droplet can receive, as well as what parameters of the plasma and beam have the main influence on this process. To answer this question, we first consider the solution of equations 1 and 2, assuming that the mass of the droplet does not change when heated. The results of solving

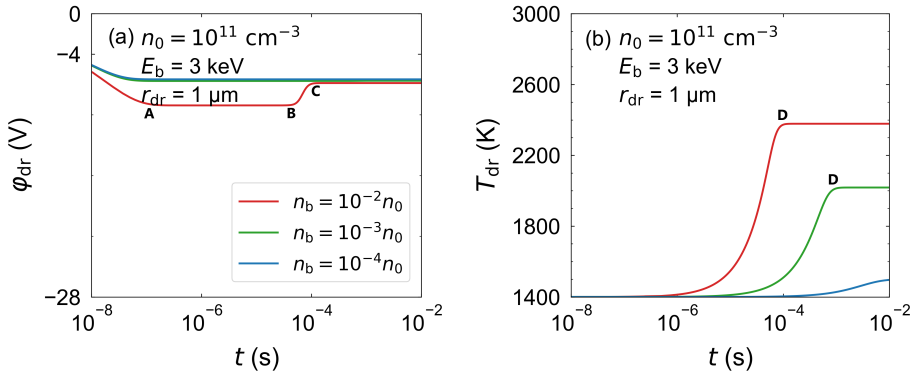


**Figure 2:** Potential and temperature dynamics of a copper droplet with radius $r_{dr} = 1\ \mu m$ for different beam and plasma density ratios ($n_0 = 10^{11}$ cm$^{-3}$, $\varepsilon_b = 3$ keV).

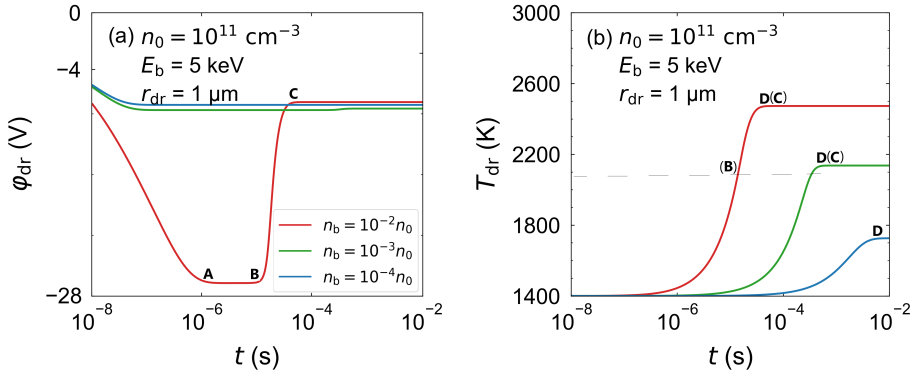


**Figure 3:** Potential and temperature dynamics of a copper droplet with radius $r_{dr} = 1\ \mu$m for different beam and plasma density ratios ($n_0 = 10^{11}$ cm$^{-3}$, $\varepsilon_b = 5$ keV).

these equations are presented in figures 2-5 (note the use of a logarithmic time-axis). Note also that the figures use the notation $E_b$ to represent electron beam energy.

Figure 2 shows the dynamics of the potential and temperature of the droplet with radius 1 $\mu$m depending on the electron beam and plasma density ratio ($n_b/n_0$), for beams with electron energies of 3 keV.

We can see that the equilibrium potential is almost independent of the beam density $n_b$ if $n_b < 0.01\ n_0$ (blue and green curves). The droplet reaches the equilibrium potential very quickly in time $\sim 10^{-8}$s and it doesn't change during droplet heating to equilibrium temperature (point D). However, if $n_b \geq 0.01\ n_0$ (red curves) the drop potential under the action of the electron beam quickly decreases (in about $10^{-7}$ sec for account of fast electrons coming to droplet and an equilibrium potential is established (point A), which does not change until the temperature reaches a critical point ($T_{cr}$), at which thermionic emission from the drop begins (point B). The potential of the droplet begins to increase (section BC) as soon as the droplet reaches $T_{cr}$, which depends on the plasma density and for a given density is about 2100 K. The growth continues until the droplet reaches its new equilibrium potential (point C) and temperature (point D).

Figure 3 shows the result when increasing the beam energy to 5 keV. Increasing the beam energy leads to a higher charging of the droplet (in longer time $\sim 10^{-6}$ sec) and as well as to a faster heating of the droplet to the critical temperature. In addition, an increase in beam energy also leads to similar processes for the case

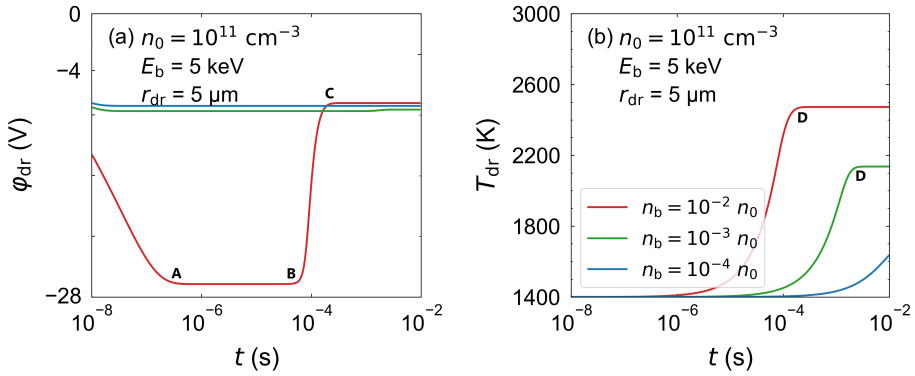


**Figure 4:** Potential and temperature dynamics of a copper droplet with radius $r_{dr} = 5$ $\mu$m for different beam and plasma density ratios ($n_0 = 10^{11}$ cm$^{-3}$, $\varepsilon_b = 5$ keV.)

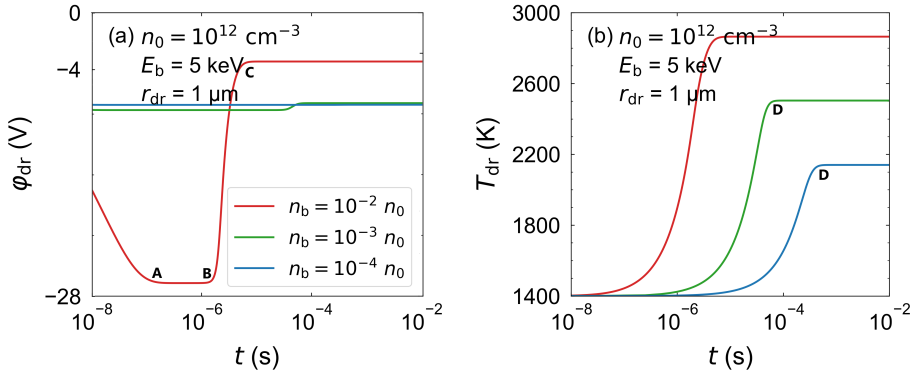


**Figure 5:** Potential and temperature dynamics of a copper droplet with radius $r_{dr} = 1$ $\mu$m for different beam and plasma density ratios ($n_0 = 10^{12}$ cm$^{-3}$, $\varepsilon_b = 5$ keV).

with a smaller density ratio (green line in 3a) and to a faster achievement of the equilibrium temperature, even for a density ratio of $10^{-4}$ (blue line in 3b). We also note that from a comparison of figures 2 and 3 it follows that an increase in the beam energy leads to a significant increase in the droplet charge, and it can be assumed that at high beam energies or high beam-to-plasma density ratios, the droplet charge can reach the Rayleigh limit and the droplet will decay, since the droplet charging time is significantly less than the time required to heat it to the critical temperature.

Figure 4 shows the development of the potential and temperature of copper droplets with a radius of 5 $\mu$m in a discharge at different ratios of the plasma and beam electron densities at a beam energy of 5 keV.

From a comparison of figures 3 and 4, it is evident that larger droplets reach the equilibrium potential faster (point A) and remain in this state longer, since they heat up more slowly and reach the critical temperature later, therefore intense thermionic emission begins later than in smaller ones (point B). It is also seen that neither the equilibrium temperature nor the potential depends on the droplet size, however, smaller droplets reach the equilibrium temperature faster.

Figure 5 shows the change in droplet potential and temperature over time at the higher plasma density ($n_0 = 10^{12}$ cm$^{-3}$) and the same electron beam energy ($\varepsilon_b = 5$ keV). One can see that in the case of a denser plasma the equilibrium temperature of the droplet increases significantly. In case where the beam density

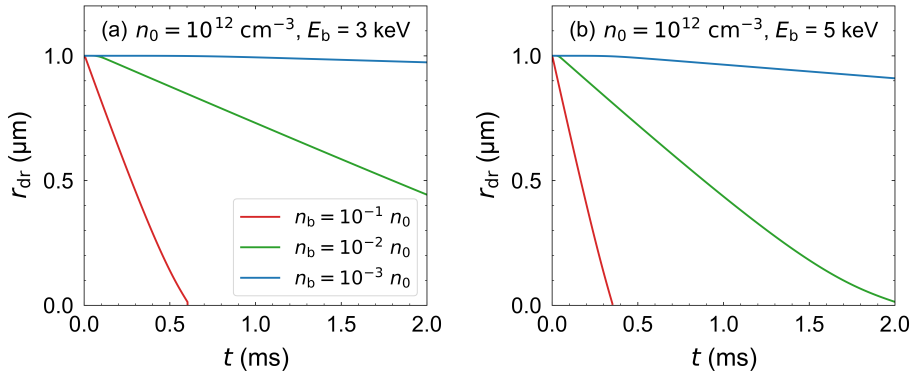


**Figure 6:** Dynamic of the droplet's radius with initial size 1 $\mu$m under electron beam for different beam and plasma density ratio. (left $\varepsilon_b$ =3 keV, right $\varepsilon_b$ = 5 keV).

is close to the plasma density ($n_b = 0.01\ n_0$), the behaviour of the potential also changes significantly: as a result of thermionic emission, it significantly exceeds the equilibrium value for cases with a lower beam density, although it still remains negative.

Thus, it can be noted that the energy and density of the beam, along with the plasma density, are parameters significantly affecting the droplet temperature. The droplet can reach a sufficiently high temperature (> 2200 K) if the electron beam density is equal or greater than $10^{-3}$ plasma density ($n_{eb} \geq 0.001\ n_0$). The higher the beam energy and plasma density, the higher the temperature the droplet can reach. The main mechanism of droplet destruction is evaporation. Thermionic emission from the droplet can prevent the droplet from reaching the critical Rayleigh charge. Rayleigh decay of the droplet is possible only if the time of development of the Rayleigh instability is less than the time of heating the droplet to the critical temperature $T_{cr}$.

Now let us find out how these parameters affect the evaporation time of a droplet and consider the solution of the system of equations 1 - 3. Figures 6 and 7 show the results of solving this system of equations for $n_0 = 10^{11}$ to $10^{12}$ cm$^{-3}$, $\varepsilon_b = 3$ keV and 5 keV, $n_b/n_0 = 0.1$ to 0.001 for droplets with an initial radius $r_{dr} = 1$ $\mu$m. The time scales in these figures represent the typical residence time of a droplet in the plasma flow ($t_{res} \sim 2$ ms) for the plasma-optical filter.

Figure 6 shows that droplets with an initial radius of 1 $\mu$m can be completely evaporated by an electron beam, even with an energy of only 3 keV, if the beam density is $\sim 0.1$ of the plasma density (red curve). At a ratio of $\sim 0.01$ (green curve), the droplet can be evaporated by increasing the beam energy to 5 keV (on the right). At a lower beam density (blue curve), the droplet will only slightly evaporate, and higher energy beams are needed. The change in droplet temperature (top) and potential (bottom) for these cases is shown in figure 7. It can be seen that the temperature of the droplets initially remains constant, but as the droplets evaporate, it begins to decrease (red curves and green curve on the right). We see that if the equilibrium temperature of the droplet is less than 2400 K, the evaporation process is very slow and the temperature of the droplet remains almost unchanged, despite the decrease in its radius by almost 50% (green curve on the left). Intensive evaporation begins if the droplet reaches a temperature of about 2400 K and higher (red curves and green curve on the right). In this case, a droplet with an initial radius of 1 $\mu$m can completely evaporate during its stay in the plasma-optical filter.

The temperature begins to decrease significantly when the radius of the droplet decreases by almost half and drops sharply (red curves) when the radius decreases by more than 90%. The droplet potential also changes during the evaporation process, as shown in figure 7 (bottom). It can be seen that, as before, the

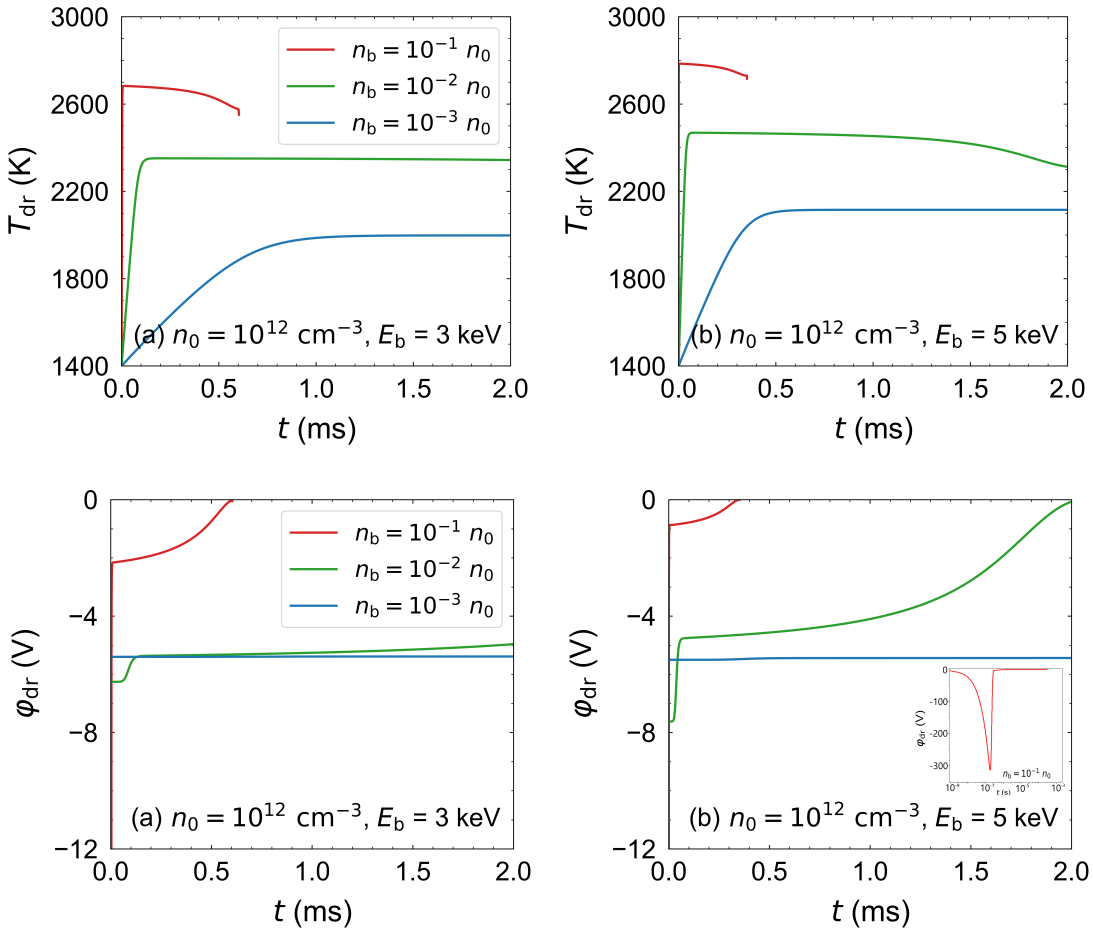


**Figure 7:** Dynamic of the droplet's temperature (top) and potential (bottom) for case present on figure 6.

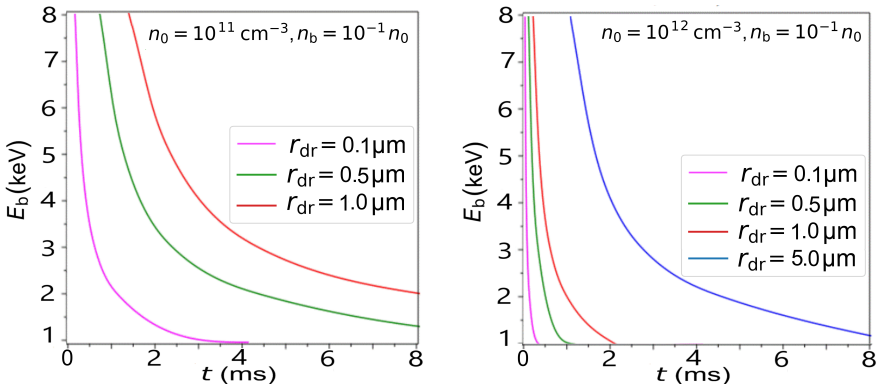


**Figure 8:** The electron beam energy required for complete evaporation of a droplet of different initial size (left $n_0 = 10^{11}$ cm$^{-3}$, right $n_0 = 10^{12}$ cm$^{-3}$, $n_b = 0.1 n_0$) in each time.

equilibrium potential remains constant (blue curves and the green curve at the bottom left) and begins to increase noticeably only when the droplet loses about 50% of its mass (green curve at the bottom left). However, if the temperature exceeds 2400 K value, the drop potential continues to increase smoothly throughout the evaporation process (red curve at the bottom and green curve at the bottom right), both due to the arrival of ions on the drop and due to electron emission processes, approaching 0, but still not reaching positive values.

For a better understanding of what beam energy is required for complete evaporation of a droplet at a certain time, we present figure 8, which shows the beam energy required for complete evaporation of droplets of different sizes at a plasma density of $10^{11}$ cm$^{-3}$ (left) and $10^{12}$ cm$^{-3}$ (right) and a beam density of $n_b = 0.1 n_0$.

We see that smaller droplets evaporate much faster than larger ones. It is also obvious that the plasma density, along with the beam density, is also an important parameter, so in a plasma with a density of $10^{12}$ cm$^{-3}$, a droplet with an initial radius of 1 $\mu$m can be completely evaporated in 2 ms by a beam with an energy of 1.5 keV, whereas in a plasma with a density of $10^{11}$ cm$^{-3}$, a beam with an energy of about 6 keV is needed for this. In addition, larger macroparticles can be completely evaporated in such plasma, if beam density is $0.1 n_0$. For example, a beam with an energy of 4 keV is needed for the complete evaporation of a droplet with a radius of 5 $\mu$m in 2 ms. In the case of a lower plasma density, a beam of significantly greater energy is required (> 8 keV) to evaporate such a drop at the same time.

Figure 9 shows the electron beam energy required to evaporate a droplet of radius 0.5 and 0.1 $\mu$m in a given time for different plasma and beam densities.

It is visible that the closer the beam density is to the plasma density, the faster the macroparticles can evaporate. As can be seen from the calculation, for the evaporation of droplets with a radius of $\leq 1 \mu m$, the beam density must be $n_{eb} \geq 0.01 n_0$. For the proposed plasma-optical filter, where the electron beam is formed self-consistently, by bombarding the ions of the inner surface of a negatively charged cylindrical electrode, we can calculate the density of the generated beam as:

$$n_b = 0.6 \frac{\gamma n_0}{v_b} \sqrt{T_e / m_i} = 0.6 \gamma n_0 \left( \frac{m_e}{m_i} \cdot \frac{T_e}{U} \right)^{1/2}, \tag{14}$$

where $\gamma$ - secondary ion-electron emission coefficient $\approx 0.1$, U is the voltage applied to the electrode. At U = 3000 eV and $T_e$ = 3 eV, we get $n_b \approx 4 \cdot 10^{-5} n_0$, which is too small for effective evaporation. But due to the fact that the mean free path of high-energy electrons is much larger than the filter diameter, their density is much greater than this value. As we showed earlier, the collision frequency of high-energy electrons

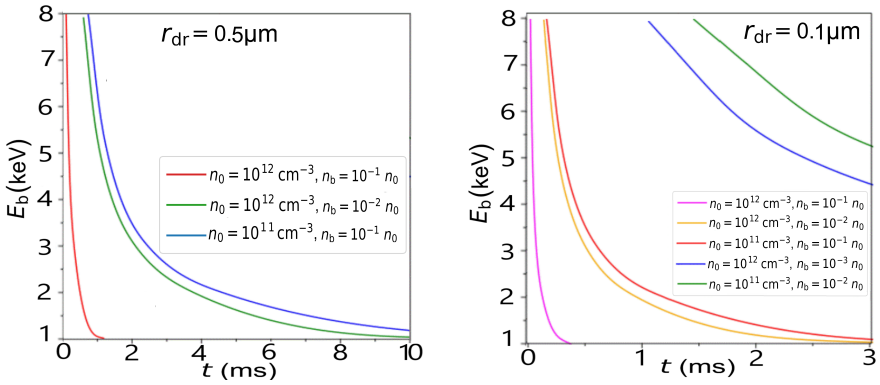


**Figure 9:** Electron beam energy needs for the complete droplet's evaporation in a giving time for different beam-plasma density ratio (on the left $r_{dr}$ = 0.5 $\mu$m, right $r_{dr}$ = 0.1 $\mu$m).

$\nu_{b-e} \approx 0.4 \cdot 10^3$ s$^{-1}$ while the inverse time during which fast electrons cross the volume of the lens is equal to $V_{eb}/D \approx 10^9$ s$^{-1}$ (D - lens diameter $\sim$ 7 cm) i.e., $\nu_{b-e} << V_{eb}/D$. Thus, high-energy electrons repeatedly cross the plasma flow transversely during the free path time and accumulate in the volume.

## 5 Conclusion

A plasma-optical filter for fragmentation and evaporation of arc plasma flow droplets is considered. The influence of energetic electrons generated as a result of secondary ion-electron emission in the plasma-optical filter on droplet evaporation in an arc plasma flow is considered. A self-consistent system of equations is formulated to describe the sublimation/evaporation of droplets in an arc plasma flow with a high density (up to $10^{12}$ cm$^{-3}$) in the presence of energetic electrons (up to 5 keV). We show exemplarily for a copper cathodic vacuum arc discharge that droplets can reach temperatures from heating by such a plasma with fast electrons up to 2700 K. The temperature that a droplet can reach does not depend on its size and is determined only by the energy and density of the electron beam and the plasma density. However, smaller droplets reach the equilibrium temperature faster than larger ones. The main mechanism of mass loss is evaporation. Although evaporation occurs at any temperature, it is more intense at high temperatures, namely, when the droplet temperature exceeds the critical temperature at which thermionic emission from the droplet begins. The evaporation time depends significantly on the equilibrium temperature of the droplet. The equilibrium temperature that a droplet can reach is determined by the energy and density of the electron beam and the plasma density. These parameters are decisive for the droplet evaporation time. There is a lower limit of the plasma density at which a droplet with a radius of about 1 $\mu$m evaporates in about 1 ms, it should be greater than $10^{11}$ cm$^{-3}$, the best result can be achieved if it is $10^{12}$ cm$^{-3}$. The simulation also showed that the closer the electron beam density to the plasma density, the shorter the evaporation time. For a satisfactory evaporation time ($\sim 2 \div 3$ ms), the beam density should be greater than 0.001 of the plasma density and such a density can be achieved in a plasma-optical filter. The simulation showed that smaller droplets evaporate faster than larger ones and require significantly less energy and electron beam density for evaporation at the same time.

## Acknowledgments

This work is supported partly by the grant DFG (Deutsche Forschungsgemeinschaft) under project number 525228371.

## References

[AVA+19] A. A. Goncharov, V. Y. Bazhenov, A. S. Bugaev, A. M. Dobrovolskiy, V. I. Gushenets, I. V. Litovko, I. V. Naiko, and E. M. Oks, Recent Progress in Development New Generation Erosion Plasma Sources, *IEEE Transactions on Plasma Science* **47** no. 8 (2019), 3594–3600. doi:10.1109/TPS.2019.2915644.

[AAS07] D. Aksenov, I. Aksenov, and V. Strelnitskiy, Vacuum-arc sources of erosion plasma with magnetic filters: review, *VANT* **90** no. 2 (2007), 190–203.

[And97] A. Anders, Growth and decay of macroparticles: A feasible approach to clean vacuum arc plasmas?, *Journal of Applied Physics* **82** no. 8 (1997), 3679–3688. doi:10.1063/1.365731.

[And99] A. Anders, Approaches to rid cathodic arc plasmas of macro- and nanoparticles: a review, *Surface and Coatings Technology* **120-121** (1999), 319–330. doi:10.1016/S0257-8972(99)00460-0.

[And00] Anders, A., *Handbook of Plasma Immersion Ion Implantation and Deposition*, John Wiley &Sons, Inc., October 2000 (Eng). Available at https://www.wiley.com/en-us/Handbook+of+Plasma+Immersion+Ion+Implantation+and+Deposition-p-9780471246985.

[Arb15] J. W. Arblaster, Thermodynamic Properties of Copper, *Journal of Phase Equilibria and Diffusion* **36** no. 5 (2015), 422–444. doi:10.1007/s11669-015-0399-x.

[BD83] G. Bader and P. Deuflhard, A semi-implicit mid-point rule for stiff systems of ordinary differential equations, *Numerische Mathematik* **41** no. 3 (1983), 373–398. doi:10.1007/BF01418331.

[BG92] R. Boxman and S. Goldsmith, Macroparticle contamination in cathodic arc coatings: generation, transport and control, *Surface and Coatings Technology* **52** (1992), 39–50. doi:10.1016/0257-8972(92)90369-L.

[BF69] I. M. Bronshtein and B. S. Fraiman, *VTORICHNAYA ELEKTRONNAYA EMISSIYA. (Secondary Electron Emission).*, Nauka, 1969. Available at https://www.osti.gov/biblio/4160985.

[FMG14] A. Fisk, V. Maslov, and A. Goncharov, Device for the Elimination of Microdroplets from a Cathodic Arc Plasma Source, June 2014, p. 8. Available at https://www.freepatentsonline.com/y2014/0034484.html.

[Gon16] A. A. Goncharov, Recent development of plasma optical systems (invited), *Review of Scientific Instruments* **87** no. 2 (2016), 02B901. doi:10.1063/1.4931718.

[Han82] E. Hantzsche, The thermo-field emission of electrons in arc discharges, *Beiträge aus der Plasmaphysik* **22** no. 4 (1982), 325–346. doi:10.1002/ctpp.19820220403.

[HS63] C. D. Hendricks and J. M. Schneider, Stability of a Conducting Droplet under the Influence of Surface Tension and Electrostatic Forces, *American Journal of Physics* **31** no. 6 (1963), 450–453. doi:10.1119/1.1969579.

[I.G94] I.G. Brown, Vacuum arc ion sources, *Review of Scientific Instruments* **65** no. 10 (1994), 3061–3081. doi:10.1063/1.1144756.

[MGM77] J. E. Mayer and M. Goeppert-Mayer, *Statistical Mechanics*, 2nd ed. ed., John Wiley & Sons Ltd., January 1977 (Eng).

[MSL26] H. M. Mott-Smith and I. Langmuir, The theory of collectors in gaseous discharges, *Phys. Rev.* **28** no. 4 (1926), 727–763. doi:10.1103/PhysRev.28.727.

[MG56] E. L. Murphy and R. H. Good, Thermionic emission, field emission, and the transition region, *Phys. Rev.* **102** no. 6 (1956), 1464–1473. doi:10.1103/PhysRev.102.1464.

[SR97] L. F. Shampine and M. W. Reichelt, The matlab ode suite, *SIAM Journal on Scientific Computing* **18** no. 1 (1997), 1–22. doi:10.1137/S1064827594276424.

[SS00] P. Siemroth and T. Schülke, Copper metallization in microelectronics using filtered vacuum arc deposition — principles and technological development, *Surface and Coatings Technology* **133-134** (2000), 106–113. doi:10.1016/S0257-8972(00)00883-5.

[SJ06] L. Spitzer Jr., *Physics of Fully Ionized Gases*, second revised edition ed., Dover Publications, July 2006. Available at https://www.book-info.com/isbn/0-486-44982-3.htm.

[Ste57] E. J. Sternglass, *THEORY OF SECONDARY ELECTRON EMISSION UNDER ELECTRON BOMBARDMENT. Scientific Paper 6-94410-2-P9*, Tech. report, Westinghouse Electric Corp. Research Labs., Pittsburgh, 1957. Available at https://www.osti.gov/biblio/4185862.

[Zim05] O. Zimmer, Vacuum arc deposition by using a Venetian blind particle filter, *Surface and Coatings Technology* **200** (2005), 440–443. doi:10.1016/j.surfcoat.2005.02.208.